mathematics

MDPI

Article

Dynamical Analysis and Optimal Control for a SEIR Model Based on Virus Mutation in WSNs

Guiyun Liu [1,†], Jieyong Chen [1,†], Zhongwei Liang [1,*], Zhimin Peng [1] and Junqiang Li [1]

School of Mechanical and Electric Engineering, Guangzhou University, Guangzhou 510006, China; liugy@gzhu.edu.cn (G.L.); 1707700074@e.gzhu.edu.cn (J.C.); 2112007150@e.gzhu.edu.cn (Z.P.); 2112007147@e.gzhu.edu.cn (J.L.)

* Correspondence: liangzhouwei@gzhu.edu.cn

† Both authors contributed equally to this work.

Abstract: With the rapid development of science and technology, the application of wireless sensor networks (WSNs) is more and more widely. It has been widely concerned by scholars. Viruses are one of the main threats to WSNs. In this paper, based on the principle of epidemic dynamics, we build a SEIR propagation model with the mutated virus in WSNs, where E nodes are infectious and cannot be repaired to S nodes or R nodes. Subsequently, the basic reproduction number R_0, the local stability and global stability of the system are analyzed. The cost function and Hamiltonian function are constructed by taking the repair ratio of infected nodes and the repair ratio of mutated infected nodes as optimization control variables. Based on the Pontryagin maximum principle, an optimal control strategy is designed to effectively control the spread of the virus and minimize the total cost. The simulation results show that the model has a guiding significance to curb the spread of mutated virus in WSNs.

Keywords: wireless sensor networks; virus mutation; stability analysis; optimal control

Citation: Liu, G.; Chen, J.; Liang, Z.; Peng, Z.; Li, J. Dynamical Analysis and Optimal Control for a SEIR Model Based on Virus Mutation in WSNs. *Mathematics* **2021**, *9*, 929. https://doi.org/10.3390/math9090929

Academic Editor: Angel Martín-del-Rey

Received: 14 March 2021
Accepted: 20 April 2021
Published: 22 April 2021

1. Introduction

1.1. Research Background

WSN is a self-organizing network system composed of a large number of sensor nodes deployed in a specific area through wireless communication [1,2]. It can achieve dynamic and real-time information monitoring, sensing and collection of monitoring objects in the network coverage area through the cooperation between nodes. WSNs are widely used in various fields, such as manufacturing, security monitoring and even military fields [3,4].

However, due to the strong openness of nodes, it is easy to be attacked by various types of viruses [5,6]. The virus against wireless devices can be transmitted directly from the device to the device using wireless communication technologies, such as Bluetooth [7–9]. Once the virus infects too many nodes in the network, it will lead to network interruption and paralysis. The virus may mutate in the computer network [10,11], its complexity and unpredictability are unmatched by the non-mutated virus, such as CIH virus. In addition, viruses may mutate in wireless sensor networks because of the similarities between computers network and WSNs. However, most of the research on the mutated virus focuses on infectious diseases [12,13].

Therefore, it is urgent and important to study the transmission of mutated virus in WSNs based on the principle of epidemic dynamics [14,15]. Through the establishment of mutated virus propagation model, we can have a deeper understanding of the mutated virus propagation behavior in the network. Then, we can take effective control and response strategies before the large-scale spread of the mutated virus, greatly reduce the harm of the mutated virus to the network.

1.2. Related Work

The establishment and dynamic analysis of virus propagation model based on WSNs has been concerned by many scholars. Kephart, J.O. and White, S.R. [16,17] first used the epidemiological model to study and predict the spread of virus in the network. Subsequently, many epidemiological models [18–20] are proposed and applied to WSNs. Due to the different characteristics and situations of infection, the models are constantly updated, and targeted epidemic models are proposed. Different authors proposed different epidemic models to study the dynamics of malicious objects propagation and control WSNs.

In the past, Mishra B.K. et al. [21] considered the effects of exposure status, vaccination and reinfection process and proposed the SEIRS-V model. However, this paper only proves the equilibrium of disease-free equilibrium. In Reference [22], Mishra B.K. and Srivastava S.K. proposed a quarantine model of worm propagation behavior and studied the stability of the model based on the basic reproduction number. The quarantine is a way to isolate infected nodes from the network so as not to infect susceptible nodes. In Reference [23], the authors studied an SLBRS computer virus model with two delays and obtain sufficient conditions for the existence of local Hopf bifurcation and the local stability. Subsequently, in Reference [24], Srivastava P.K. et al. proposed a worm propagation model (SEIQR). The model described the influence of quarantined state and recovery state on worm propagation. Moreover, they found the equilibrium point in disease-free and endemic cases, and proved the local stability and global stability, respectively. Besides, on the basis of the SEIQR model, Mishra B.K. and Tyagi I [25] added the vaccination and proposed SEIQRS-V model. Based on the SIR model, Zhu L. et al. [26] studied the nonlinear propagation model of malware and obtained the sufficient conditions for the existence of Hopf bifurcation and the local stability.

In recent years, the authors of Reference [27] proposed the SEIRS-D agent-based model and the characteristics of the model can be adjusted to more realistic values based on the environment by integrating new elements. Huang D.W. et al. [28] proposed a model with patch injection mechanism (SIPS) to evaluate the performance of patch injection rate in inhibiting computer infection. In Reference [29], the authors considered the communication radius and distribution density of nodes and proposed a delayed SEIQRS-V model. In addition, they obtained the sufficient conditions for the local stability and the existence of Hopf bifurcation. In addition, a variety of models have been proposed, such as SILRD [30], I2S2R [31], SEIQRV [32], VCQPS [33], etc.

In reality, after a period of time, the virus will be included in the database of the anti-virus program. Then, it will be intercepted by the anti-virus program and lose its infectivity. However, in order to continue spreading the virus, the virus maker will also update the virus. Therefore, it is necessary to study and control the mutated virus in the network. However, most of the researches on mutated viruses focus on how to detect them. As early as in [34], the authors proposed a computer virus detection method based on neural network, which can detect and destroy the mutated virus. In Reference [11], EVs and ECs are proposed to detect and analyze computer viruses for the first time. This method can effectively detect all mutations of corresponding viruses with one signature. In Reference [35], Rad B.B. developed a Hidden Markov Model that can recognize and detect other mutations in the same metamorphic virus family. It is rare to study the propagation behavior of mutated virus in the network. This paper enriches the content of this aspect.

In this paper, we will apply the theories of epidemic dynamics and optimal control to study the security of WSNs. Optimal control [36–38], as a method of studying the optimal dynamic strategy, has also been widely applied in wireless sensor networks. In Reference [39], the attack behavior of malicious programs is studied by combining the epidemic model and the loss equation. The maximum attack behavior of virus is discussed by taking the node communication radius and the media scanning rate as the optimal control variables. In Reference [40], the best defense strategy model between malware and WSNs is constructed and it can achieve the best defense effect with less resource consumption. In Reference [41], Huang Y.H. et al. proposed an anti-virus weight

adaptive strategy, which effectively alleviated the spread of the virus in the network. In Reference [26], the optimal dynamic strategy for the system and malware based on Pontryagin Maximum Principle is given and it can reduce the total cost and inhibit the spread of malware to a certain extent.

1.3. Contributions

This paper is the first time to apply mutation model to WSNs to study the spread and control of virus, and proposes an SEIR epidemic model based on virus mutation in WSNs. Our contributions are as follows:

1. An SEIR model based on virus mutation is established to describe the propagation process of mutated virus in WSNs.
2. Calculating the basic reproduction number R_0 of the improved model by the next generation matrix method. Besides, the local and global stability of the two equilibria are proved and simulated by the Routh criterion and the Lyapunov stability method. Moreover, the influence of the repair rate γ_1 and γ_2 on the basic reproduction number is also revealed in the simulation part.
3. Based on the Pontryagin maximum principle, the optimal control variable pairs of the repair ratio of infected nodes and the repair ratio of mutated infected nodes are obtained. The simulation results show that the optimal control strategy ensures the security of wireless sensor networks and minimizes the maintenance cost.

The rest of the paper is as follows. The compositions of the model are introduced in Section 2. The local and global stability is proved and the optimal strategy is designed in Section 3. The simulation results, which support our theoretical predictions, are shown in Section 4. The relevant conclusions are given in Section 5.

2. Modeling

2.1. Dynamic Equation

The proposed model is global and deterministic, and the sensor nodes are divided into six parts: susceptible (S), exposed (E), infected (I_1), mutated infected (I_2), recovered (R) and death (D). The relationship between the six compartments is depicted in Figure 1. S nodes are vulnerable to viruses; E nodes are compromised with the attacker, but they work normally; I_1 nodes transform from E nodes, but they are unable to work normally; I_2 nodes are obtained by virus mutation from I_1 nodes, they are also unable to work normally; R nodes are immune to both pre mutated and post mutated viruses; D nodes are completely damaged. Specifically, E, I_1 and I_2 nodes all can infect other nodes. Now, let us make the following assumptions.

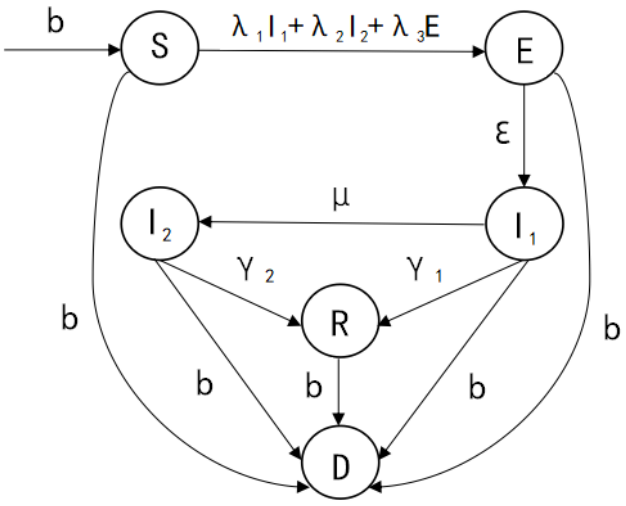

Figure 1. Flow chart of the infectious disease model.

The number of nodes increases at rate b, they all belong to S nodes. Meanwhile, new E nodes are generated with $\lambda_1 I_1(t)S(t)$, $\lambda_2 I_2(t)S(t)$ and $\lambda_3 E(t)S(t)$. The parameters λ_1, λ_2 and λ_3 represent the transmission rate of I_1, I_2 and E nodes, respectively. Because E nodes are mainly latent and the mutated virus is more infectious, λ_2 is greater than λ_1 and λ_1 is greater than λ_3. E nodes are converted to I_1 nodes at rate ε, and I_1 nodes mutate to I_2 nodes at rate μ. Because I_1 and I_2 nodes are unable to work normally, they can be detected by the anti-virus program, and repaired at rate γ_1 and γ_2, respectively. In addition, the five compartments S, E, I_1, I_2 and R have the same mortality b. All parameters are greater than 0. The parameters are summarized in Table 1.

Table 1. The parameters of the model.

Symbol	Description
b	Birth rate or Death rate
λ_1	Transmission rate of I_1 nodes
λ_2	Transmission rate of I_2 nodes
λ_3	Transmission rate of E nodes
ε	Probability at which E nodes are converted to I_1 nodes
μ	Probability of virus mutation
γ_1	Repair rate of I_1 nodes
γ_2	Repair rate of I_2 nodes

$S(t)$, $E(t)$, $I_1(t)$, $I_2(t)$, and $R(t)$ are the ratio of susceptible, exposed, infected, mutated infected and recovered nodes at t. The novel dynamical system is given as follows:

$$\begin{cases} \frac{dS(t)}{dt} = b - bS(t) - \lambda_1 S(t)I_1(t) - \lambda_2 S(t)I_2(t) - \lambda_3 S(t)E(t), \\ \frac{dE(t)}{dt} = \lambda_1 S(t)I_1(t) + \lambda_2 S(t)I_2(t) + \lambda_3 S(t)E(t) - (\varepsilon + b)E(t), \\ \frac{dI_1(t)}{dt} = \varepsilon E(t) - (\gamma_1 + b + \mu)I_1(t), \\ \frac{dI_2(t)}{dt} = \mu I_1(t) - (\gamma_2 + b)I_2(t), \\ \frac{dR(t)}{dt} = \gamma_1 I_1(t) + \gamma_2 I_2(t) - bR(t), \\ \frac{dD(t)}{dt} = bS(t) + bE(t) + bI_1(t) + bI_2(t) + bR(t). \end{cases} \tag{1}$$

Because $R(t)$ and $D(t)$ are independent of the other four equations, the following system is considered:

$$\begin{cases} \frac{dS(t)}{dt} = b - bS(t) - \lambda_1 S(t)I_1(t) - \lambda_2 S(t)I_2(t) - \lambda_3 S(t)E(t), \\ \frac{dE(t)}{dt} = \lambda_1 S(t)I_1(t) + \lambda_2 S(t)I_2(t) + \lambda_3 S(t)E(t) - (\varepsilon + b)E(t), \\ \frac{dI_1(t)}{dt} = \varepsilon E(t) - (\gamma_1 + b + \mu)I_1(t), \\ \frac{dI_2(t)}{dt} = \mu I_1(t) - (\gamma_2 + b)I_2(t). \end{cases} \tag{2}$$

For the system (2), we suppose that $N(t) = S(t) + E(t) + I_1(t) + I_2(t)$ and it satisfies

$$\frac{dN(t)}{dt} = b - bN(t) - \gamma_1 I_1(t) - \gamma_2 I_2(t), \tag{3}$$

which implies $\frac{dN(t)}{dt} \leq b - bN(t)$, thus $\limsup_{t\to\infty} N(t) \leq 1$. Also, if $N(t) > 1$ then $\dot{N}(t) < 0$. Therefore, we get $0 < N \leq 1$. we get a feasible region as follow:

$$D = \left\{ (S(t), E(t), I_1(t), I_2(t)) \in \mathrm{R}_+^4 : 0 < S(t) + E(t) + I_1(t) + I_2(t) \leq 1 \right\}. \tag{4}$$

Therefore, the solution of system (2) is bounded and independent of the initial condition. Therefore, D is an invariant set. In addition, $0 < N \leq 1$, D also is a positive set. Therefore, we will consider the stability of system (2) on the set D

2.2. Calculation of the Equilibrium Point and the Basic Reproduction Number

In this subsection, two equilibrium points of the system (2) on the set D are calculated.

The first point is the disease-free equilibrium point $N(t) = S(t) + E(t) + I_1(t) + I_2(t)$ $P^0 = (S^0,\ E^0,\ {I_1}^0,\ {I_2}^0)$, and

$$S^0 = 1,\ E^0 = 0,\ {I_1}^0 = 0,\ {I_2}^0 = 0. \tag{5}$$

The second point is the endemic equilibrium point $P^* = (S^*,\ E^*,\ {I_1}^*,\ {I_2}^*)$, and

$$S^* = \frac{(\gamma_1 + b + \mu)(\gamma_2 + b)(\varepsilon + b)}{\lambda_1\varepsilon(\gamma_2 + b) + \lambda_2\varepsilon\mu + \lambda_3(\gamma_1 + b + \mu)(\gamma_2 + b)}, \tag{6}$$

$$E^* = \frac{\lambda_1 b\varepsilon(\gamma_2 + b) + \lambda_2 b\varepsilon\mu + \lambda_3 b(\gamma_1 + b + \mu)(\gamma_2 + b) - b(\gamma_1 + b + \mu)(\gamma_2 + b)(\varepsilon + b)}{\varepsilon(\gamma_2 + b)(\varepsilon + b)\left[\lambda_1 + \frac{\lambda_2\mu}{\gamma_2 + b} + \frac{\lambda_3(\gamma_1 + b + \mu)}{\varepsilon}\right]}, \tag{7}$$

$${I_1}^* = \frac{\lambda_1 b\varepsilon(\gamma_2 + b) + \lambda_2 b\varepsilon\mu + \lambda_3 b(\gamma_1 + b + \mu)(\gamma_2 + b) - b(\gamma_1 + b + \mu)(\gamma_2 + b)(\varepsilon + b)}{(\gamma_1 + b + \mu)(\gamma_2 + b)(\varepsilon + b)\left[\lambda_1 + \frac{\lambda_2\mu}{\gamma_2 + b} + \frac{\lambda_3(\gamma_1 + b + \mu)}{\varepsilon}\right]}, \tag{8}$$

$${I_2}^* = \frac{\mu[\lambda_1 b\varepsilon(\gamma_2 + b) + \lambda_2 b\varepsilon\mu + \lambda_3 b(\gamma_1 + b + \mu)(\gamma_2 + b) - b(\gamma_1 + b + \mu)(\gamma_2 + b)(\varepsilon + b)]}{(\gamma_1 + b + \mu)(\gamma_2 + b)^2(\varepsilon + b)\left[\lambda_1 + \frac{\lambda_2\mu}{\gamma_2 + b} + \frac{\lambda_3(\gamma_1 + b + \mu)}{\varepsilon}\right]}. \tag{9}$$

Furthermore, by the next generation matrix method, the basic reproduction number R_0 is obtained.

Set

$$F = \begin{bmatrix} \lambda_3 & \lambda_1 & \lambda_2 \\ 0 & 0 & 0 \\ 0 & 0 & 0 \end{bmatrix} \tag{10}$$

and

$$V = \begin{bmatrix} \varepsilon + b & 0 & 0 \\ -\varepsilon & \gamma_1 + b + \mu & 0 \\ 0 & -\mu & \gamma_2 + b \end{bmatrix}. \tag{11}$$

The next generation matrix is FV^{-1}, the basic reproduction number R_0 is its spectral radius.

$$FV^{-1} = \begin{bmatrix} \frac{\lambda_1\varepsilon(\gamma_2+b)+\lambda_2\varepsilon\mu+\lambda_3(\gamma_1+b+\mu)(\gamma_2+b)}{(\gamma_1+b+\mu)(\gamma_2+b)(\varepsilon+b)} & \frac{\lambda_1(\gamma_2+b)+\lambda_2\mu}{(\gamma_1+b+\mu)(\gamma_2+b)} & \frac{\lambda_2}{(\gamma_2+b)} \\ 0 & 0 & 0 \\ 0 & 0 & 0 \end{bmatrix}, \tag{12}$$

$$R_0 = \frac{\lambda_1\varepsilon(\gamma_2 + b) + \lambda_2\varepsilon\mu + \lambda_3(\gamma_1 + b + \mu)(\gamma_2 + b)}{(\gamma_1 + b + \mu)(\gamma_2 + b)(\varepsilon + b)}. \tag{13}$$

3. Dynamic Analysis and Optimal Strategy

In this section, the local and global stability of two equilibrium points are proved by using the Routh criterion [42] and the Lyapunov stability method [43]. The existence of local stability and global stability indicates that the development of this infectious disease will not appear large-scale repeated infection, and will eventually maintain a static equilibrium with the passage of time. Moreover, based on Pontryagin maximum principle [44], an optimal strategy is proposed to control the spread of virus with minimum cost.

3.1. Subs Stability Analysis of P^0

Theorem 1. *When $R_0 < 1$, the disease-free equilibrium point P^0 is locally asymptotically stable.*

Proof. First, we can get the disease-free equilibrium point $P^0 = (1, 0, 0, 0)$ according to the system (2). Thus, the Jacobian matrix of the disease-free equilibrium point P^0 is:

$$J\left(P^0\right) = \begin{bmatrix} -b & -\lambda_3 & -\lambda_1 & -\lambda_2 \\ 0 & -\varepsilon - b & \lambda_1 & \lambda_2 \\ 0 & \varepsilon & -\gamma_1 - b - \mu & 0 \\ 0 & 0 & \mu & -\gamma_2 - b \end{bmatrix} \tag{14}$$

Thus, $-b$ is one of the eigenvalues of $J(P^0)$, so just consider the following Jacobian matrix:

$$J'\left(P^0\right) = \begin{bmatrix} -\varepsilon - b & \lambda_1 & \lambda_2 \\ \varepsilon & -\gamma_1 - b - \mu & 0 \\ 0 & \mu & -\gamma_2 - b \end{bmatrix} \tag{15}$$

The characteristic polynomial of (15) is

$$P(\lambda) = a_3\lambda^3 + a_2\lambda^2 + a_1\lambda + a_0 \tag{16}$$

where

$$a_3 = 1 > 0, \tag{17}$$

$$a_2 = 3b + \gamma_1 + \gamma_2 + \mu + \varepsilon > 0, \tag{18}$$

$$a_1 = \frac{\lambda_1\varepsilon(\gamma_2 + b)(1 - R_0) + \lambda_2\varepsilon\mu + \lambda_3(\gamma_1 + b + \mu)(\gamma_2 + b)}{R_0(\gamma_2 + b)} + (\gamma_1 + b + \mu)(\gamma_2 + b) + (\varepsilon + b)(\gamma_2 + b) > 0, \tag{19}$$

and

$$a_0 = \frac{(1 - R_0)[\lambda_1\varepsilon(\gamma_2 + b) + \lambda_2\varepsilon\mu] + \lambda_3(\gamma_1 + b + \mu)(\gamma_2 + b)}{R_0} > 0. \tag{20}$$

Moreover, a simple calculation shows $a_1a_2 - a_0 > 0$. Thus, according to the Routh criterion, P^0 is locally asymptotically stable if $R_0 < 1$. □

Theorem 2. *When $R_0 < 1$, the disease-free equilibrium point P^0 is globally asymptotically stable.*

Proof. We can prove it by the Lyapunov stability method. Consider the following Lyapunov function:

$$V(t) = S(t) - 1 - \ln S(t) + E(t) + \frac{\lambda_1(\gamma_2 + b) + \lambda_2\mu}{(\gamma_1 + b + \mu)(\gamma_2 + b)} I_1(t) + \frac{\lambda_2}{\gamma_2 + b} I_2(t) > 0. \tag{21}$$

We have:

$$\begin{aligned} \tfrac{dV(t)}{dt} &= -b\left[S(t) + \tfrac{1}{S(t)} - 2\right] + \lambda_1 I_1(t) + \lambda_2 I_2(t) + \lambda_3 E(t) - (\varepsilon + b)E(t) + \\ &\quad \tfrac{\lambda_1(\gamma_2+b)+\lambda_2\mu+\frac{\lambda_3(\gamma_1+b+\mu)(\gamma_2+b)}{\varepsilon}-\frac{\lambda_3(\gamma_1+b+\mu)(\gamma_2+b)}{\varepsilon}}{(\gamma_1+b+\mu)(\gamma_2+b)}[\varepsilon E(t) - (\gamma_1 + b + \mu)I_1(t)] + \\ &\quad \tfrac{\lambda_2}{(\gamma_2+b)}[\mu I_1(t) - (\gamma_2 + b)I_2(t)] \\ &= -b\left[S(t) + \tfrac{1}{S(t)} - 2\right] - (\varepsilon + b)E(t) + \tfrac{\lambda_1(\gamma_2+b)+\lambda_2\mu+\frac{\lambda_3(\gamma_1+b+\mu)(\gamma_2+b)}{\varepsilon}}{(\gamma_1+b+\mu)(\gamma_2+b)}\varepsilon E(t) \\ &= -b\left[S(t) + \tfrac{1}{S(t)} - 2\right] - (\varepsilon + b)\left[1 - \tfrac{\lambda_1(\gamma_2+b)+\lambda_2\mu+\frac{\lambda_3(\gamma_1+b+\mu)(\gamma_2+b)}{\varepsilon}}{(\gamma_1+b+\mu)(\gamma_2+b)(\varepsilon+b)}\varepsilon\right]E(t) \\ &= -b\left[S(t) + \tfrac{1}{S(t)} - 2\right] - (\varepsilon + b)(1 - R_0)E(t) \end{aligned} \tag{22}$$

According to mean inequality $\sqrt[n]{a_1a_2\cdots a_n} \leq \frac{a_1+a_2+\cdots+a_n}{n}$, $S(t) + \frac{1}{S(t)} \geq 2$. Then, $\frac{dV(t)}{dt} \leq 0$ if $R_0 \leq 1$. It is noted that $\frac{dV(t)}{dt}|_{P^0} = 0$. According to the Lyapunov stability theorem, P^0 is globally asymptotically stable. □

3.2. Stability Analysis of P*

Theorem 3. *When $R_0 > 1$, the epidemic equilibrium point P * is locally asymptotically stable.*

Proof. First of all, S^*, E^*, $I_1{}^*$ and $I_2{}^*$ are given in Equations (4)–(7). Thus, the Jacobian matrix at the epidemic equilibrium P^* is:

$$J(P^*) = \begin{bmatrix} -\lambda_1 I_1{}^* - \lambda_2 I_2{}^* - \lambda_3 E^* - b & -\lambda_3 S^* & -\lambda_1 S^* & -\lambda_2 S^* \\ \lambda_1 I_1{}^* + \lambda_2 I_2{}^* + \lambda_3 E^* & -\varepsilon - b & \lambda_1 S^* & \lambda_2 S^* \\ 0 & \varepsilon & -(\gamma_1 + b + \mu) & 0 \\ 0 & 0 & \mu & -(\gamma_2 + b) \end{bmatrix}. \quad (23)$$

The characteristic polynomial of Equation (13) is

$$P^*(\lambda) = a_4{}^* \lambda^4 + a_3{}^* \lambda^3 + a_2{}^* \lambda^2 + a_1{}^* \lambda + a_0{}^*. \quad (24)$$

where

$$a_4{}^* = 1 > 0, \quad (25)$$

$$a_3{}^* = bR_0 + 3b + \gamma_1 + \gamma_2 + \varepsilon + \mu > 0, \quad (26)$$

$$a_1{}^* = bR_0(\delta_1 + \delta_2) + \frac{\lambda_3(\gamma_1 + b + \mu)(\gamma_2 + b)}{R_0} + \frac{b(R_0 - 1)[\lambda_3(\gamma_1 + \gamma_2 + 2b + \mu) + \lambda_1 \varepsilon]}{R_0} > 0, \quad (27)$$

and

$$a_0{}^* = b(R_0 - 1)(\gamma_1 + b + \mu)(\gamma_2 + b)(\varepsilon + b) + \lambda_3 b(\gamma_1 + b + \mu)(\gamma_2 + b) > 0. \quad (28)$$

where

$$\delta_1 = (\gamma_2 + b)(\varepsilon + b) + (\gamma_1 + b + \mu)(\gamma_2 + b), \quad (29)$$

$$\delta_2 = \frac{\lambda_2 \varepsilon \mu + \lambda_3(\gamma_1 + b + \mu)(\gamma_2 + b)}{R_0(\gamma_2 + b)}. \quad (30)$$

In addition, a simple calculation shows $a_1{}^* a_2{}^* a_3{}^* - a_1{}^{*2} - a_0{}^* a_3{}^{*2} > 0$ and $a_2{}^* a_3{}^* - a_1{}^* > 0$. Thus, if $R_0 > 1$, according to the Routh criterion, P^* is locally asymptotically stable.

Theorem 4. *When $R_0 > 1$, the epidemic equilibrium point P* is globally asymptotically stable.*

Proof. In this subsection, S, E, I_1, I_2, R and V denote $S(t)$, $E(t)$, $I_1(t)$, $I_2(t)$, $R(t)$ and $V(t)$, respectively. Consider the following Lyapunov function:

$$\begin{aligned} V = {} & S - S^* - S^* \ln \tfrac{S}{S^*} + E - E^* - E^* \ln \tfrac{E}{E^*} + \tfrac{\varepsilon + b - \lambda_3 S^*}{\varepsilon} \left(I_1 - I_1{}^* - I_1{}^* \ln \tfrac{I_1}{I_1{}^*} \right) \\ & + \tfrac{\lambda_2 S^*}{\gamma_2 + b} \left(I_2 - I_2{}^* - I_2{}^* \ln \tfrac{I_2}{I_2{}^*} \right) \end{aligned} \quad (31)$$

For simplicity, let $t_0 = \frac{S}{S^*}$, $t_1 = \frac{E}{E^*}$, $t_2 = \frac{I_1}{I_1^*}$ and $t_3 = \frac{I_2}{I_2^*}$, we obtain:

$$\begin{aligned} \tfrac{dV}{dt} = {} & b + bS^* + (\varepsilon + b)E^* + \tfrac{\varepsilon + b - \lambda_3 S^*}{\varepsilon}(\gamma_1 + b + \mu) I_1^* + \lambda_2 S^* I_2^* \\ & - (bS^* + \lambda_3 S^* E^*) t_0 - b \tfrac{1}{t_0} - (\varepsilon + b - \lambda_3 S^*) E^* \tfrac{t_1}{t_2} - \tfrac{\lambda_2 \mu S^* I_1^*}{\gamma_2 + b} \tfrac{t_2}{t_3} \\ & - \lambda_1 S^* I_1{}^* \tfrac{t_0 t_2}{t_1} - \lambda_2 S^* I_2{}^* \tfrac{t_0 t_3}{t_1} \end{aligned} \quad (32)$$

By substituting Equations (4)–(7) in (32), we can get

$$\begin{aligned}\frac{dV}{dt} &= 2(bS^* + \lambda_3 S^* E^*) + 3\lambda_1 S^* {I_1}^* + 4\lambda_2 S^* {I_2}^* - (bS^* + \lambda_3 S^* E^*)t_0 \\ &\quad - (bS^* + \lambda_1 S^* {I_1}^* + \lambda_2 S^* {I_2}^* + \lambda_3 S^* E^*)\frac{1}{t_0} - (\lambda_1 S^* {I_1}^* + \lambda_2 S^* {I_2}^*)\frac{t_1}{t_2} \\ &\quad - \lambda_2 S^* {I_2}^* \frac{t_2}{t_3} - \lambda_1 S^* {I_1}^* \frac{t_0 t_2}{t_1} - \lambda_2 S^* {I_2}^* \frac{t_0 t_3}{t_1} \\ &= -(bS^* + \lambda_3 S^* E^*)\left(t_0 + \frac{1}{t_0} - 2\right) - \lambda_1 S^* {I_1}^* \left(\frac{1}{t_0} + \frac{t_0 t_2}{t_1} + \frac{t_1}{t_2} - 3\right) \\ &\quad - \lambda_2 S^* {I_2}^* \left(\frac{1}{t_0} + \frac{t_1}{t_2} + \frac{t_2}{t_3} + \frac{t_0 t_3}{t_1} - 4\right)\end{aligned} \tag{33}$$

According to mean inequality $\sqrt[n]{a_1 a_2 \cdots a_n} \leq \frac{a_1 + a_2 + \cdots + a_n}{n}$, $t_0 + \frac{1}{t_0} \geq 2$, $\frac{1}{t_0} + \frac{t_0 t_2}{t_1} + \frac{t_1}{t_2} \geq 3$ and $\frac{1}{t_0} + \frac{t_1}{t_2} + \frac{t_2}{t_3} + \frac{t_0 t_3}{t_1} \geq 4$ are obtained. Then $\frac{dV}{dt} \leq 0$ if $R_0 \geq 1$. According to the Lyapunov stability theorem, the epidemic equilibrium is globally asymptotically stable. □

3.3. Optimal Strategy

In this paper, our goal is not only to effectively control the spread of the virus, but also to make the cost of sensor node repair as low as possible. Selecting the repair rate of I_1 nodes γ_1 and the repair rate of I_2 nodes γ_2 as the control variable, the cost function is as follows:

$$J(\gamma_1, \gamma_2) = \min_{\gamma_1, \gamma_2} \left\{ E\left(t_f\right) + I_1\left(t_f\right) + I_2\left(t_f\right) + \int_0^{t_f} \left(c_1 {\gamma_1}^2(t) {I_1}^2(t) + c_2 {\gamma_2}^2(t) {I_2}^2(t)\right) \quad dt \right\}, \tag{34}$$

In this formula, c_1 and c_2 indicate the repair cost parameter of I_1 nodes and I_2 nodes, respectively. Here, t_f represents the terminal moment. The terms $c_1 {\gamma_1}^2(t) {I_1}^2(t)$ and $c_2 {\gamma_2}^2(t) {I_2}^2(t)$ describe the repair cost of I_1 nodes and I_2 nodes at time t. The Equation (34) shows that the sum of the number of E nodes, I_1 nodes and I_2 nodes at the terminal moment and the cost from the start time to the terminal moment is the least by controlling $\gamma_1(t)$ and $\gamma_2(t)$. We apply the Pontryagin maximum principle to solve the optimization problem and consider the following Hamiltonian:

$$H = c_1 {\gamma_1}^2(t) {I_1}^2(t) + c_2 {\gamma_2}^2(t) {I_2}^2(t) + \beta_1(t)\dot{S}(t) + \beta_2(t)\dot{E}(t) + \beta_3(t)\dot{I}_1(t) + \beta_4(t)\dot{I}_2(t), \tag{35}$$

where $\beta(t) = \{\beta_1(t), \beta_2(t), \beta_3(t), \beta_4(t)\}$ is a set of covariates. According to the Pontryagin Maximum Principle, the differential equations of covariates can be obtained as follow:

$$\begin{cases} \dot{\beta_1}(t) = [\beta_1(t) - \beta_2(t)][\lambda_1 I_1(t) + \lambda_2 I_2(t) + \lambda_3 E(t)] + b\beta_1(t) \\ \dot{\beta_2}(t) = [\beta_1(t) - \beta_2(t)]\lambda_3 S(t) + b\beta_2(t) \\ \dot{\beta_3}(t) = -2c_1 I_1(t) {\gamma_1}^2(t) + [\beta_1(t) - \beta_2(t)]\lambda_1 S(t) + (\gamma_1 + b + \mu)\beta_3(t) - \mu\beta_4(t) \\ \dot{\beta_4}(t) = -2c_2 I_2(t) {\gamma_2}^2(t) + [\beta_1(t) - \beta_2(t)]\lambda_2 S(t) + (\gamma_2 + b)\beta_4(t) \end{cases}, \tag{36}$$

where $\beta_1\left(t_f\right) = 0$ and $\beta_2\left(t_f\right) = \beta_3\left(t_f\right) = \beta_4\left(t_f\right) = 1$.

According to the Pontryagin Maximum Principle, we get

$$\begin{cases} \frac{\partial H}{\partial \gamma_1(t)} = 2c_1 \gamma_1(t) {I_1}^2(t) - \beta_3(t) I_1(t) = 0, \\ \frac{\partial H}{\partial \gamma_2(t)} = 2c_2 \gamma_2(t) {I_2}^2(t) - \beta_4(t) I_2(t) = 0. \end{cases} \tag{37}$$

From the Equation (38), it can be concluded that:

$$\gamma_1(t) = \frac{\beta_3(t)}{2c_1 I_1(t)}, \gamma_2(t) = \frac{\beta_4(t)}{2c_2 I_2(t)}. \tag{38}$$

And $\gamma_1(t), \gamma_2(t) \in [0, 1]$, so the optimal control pairs are as follows:

$$\gamma_1 * (t) = \min\left\{ \max\left(0, \frac{\beta_3(t)}{2c_1 I_1(t)}\right), \quad 1 \right\}, \gamma_2 * (t) = \min\left\{ \max\left(0, \frac{\beta_4(t)}{2c_2 I_2(t)}\right), \quad 1 \right\}. \tag{39}$$

4. Simulation

This section will be divided into three parts, the first two parts are to further verify the stability of the system, and the latter part is to show the effectiveness of the optimal control. Simulation parameters are obtained by simulating different scenes.

4.1. Stable Analysis of Disease-Free Equilibrium

In this subsection, we suppose $\lambda_1 = 0.1$, $\lambda_2 = 0.2$, $\lambda_3 = 0.05$, $\gamma_1 = 0.1$, $\gamma_2 = 0.05$, $\mu = 0.05$, $\varepsilon = 0.05$, and $b = 0.1$. According to the Formula (11), we can get $R_0 = 0.56 < 1$. Theoretically, $S(\infty) = 1$, $E(\infty) = 0$, $I_1(\infty) = 0$, and $I_2(\infty) = 0$ according to the Formula (3). The simulation results are illustrated in Figure 2, and it is consistent with Theorems 1 and 2.

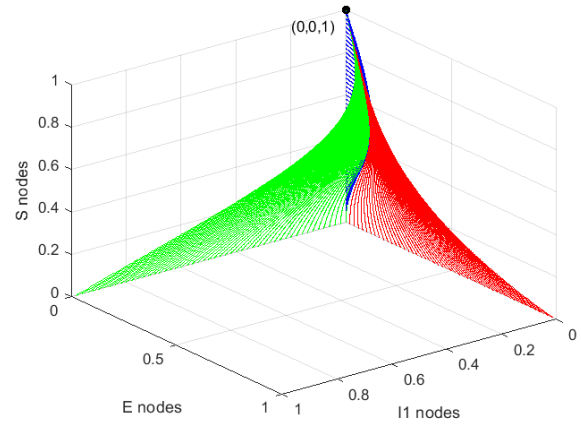

(**a**) The evolution of S, E and I_1 nodes

(Start from the X, Y and Z axis)

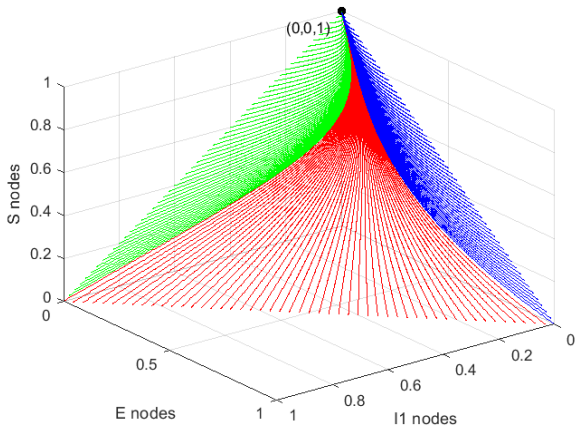

(**b**) The evolution of S, E and I_1 nodes

(Start from the hypotenuse)

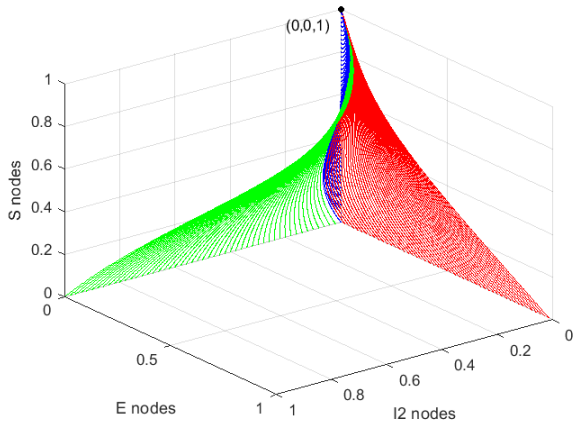

(**c**) The evolution of S, E and I_2 nodes

(Start from the X, Y and Z axis)

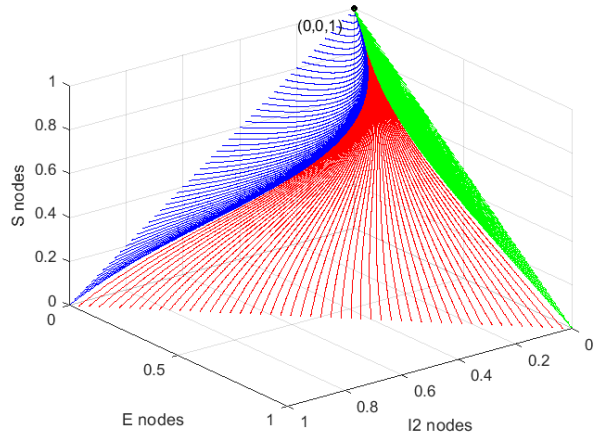

(**d**) The evolution of S, E and I_2 nodes

(Start from the hypotenuse)

Figure 2. The evolution of state variables when $R_0 < 1$.

In Figure 2a,c, the curves all start from the X, Y and Z axes, and the curves in Figure 2b,d all start from the hypotenuse of the X-Y, X-Z and Y-Z planes.

As shown in Figure 2a,b in the three-dimensional graph with I_1 nodes scale as X axis, E nodes scale as Y axis and S nodes scale as Z axis, the curves finally converge to (0, 0, 1). In Figure 2a, there are only I_1 and I_2 nodes in the beginning if the curves start from the X-axis; there are only E and I_2 nodes in the beginning if the curves start from the Y-axis;

and there are only S and I_2 nodes in the beginning if the curves start from the *Z*-axis. These assumptions ensure that the virus exists at the beginning. In Figure 2b, the ratio sum of I_1 nodes and E nodes is 1 in the X-Y plane at the initial moment; the ratio sum of I_1 nodes and S nodes is 1 in the *X*-*Z* plane at the initial moment; and the ratio sum of *E* nodes and S nodes is 1 in the *Y*-*Z* plane at the initial moment.

Figure 2c,d are similar to Figure 2a,b. In the three-dimensional graph with I_2 nodes scale as *X*-axis, *E* nodes scale as *Y*-axis and *S* nodes scale as *Z*-axis, the curves finally converge to (0, 0, 1). In Figure 2c, in the beginning, there contain only I_2 and I_1 nodes when the curves start from the *X*-axis; there contain only *E* and I_1 nodes when the curves start from the *Y*-axis; and there contain only *S* and I_1 nodes when the curves start from the *Z*-axis. In Figure 2d, the curves contain only I_2 and *E* nodes in the *X*-*Y* plane; the curves contain only I_2 and *S* nodes in the *X*-*Z* plane; and the curves contain only *E* and *S* nodes in the *Y*-*Z* plane. In summary, those curves will gather together, and then finally converge to (0, 0, 1) in a variety of cases of $R_0 < 1$, as shown in Figure 2. These results are according to Theorems 1 and 2.

4.2. Stable Analysis of Epidemic Equilibrium

In this subsection, $\lambda_1 = 0.2$, $\lambda_2 = 0.3$, $\lambda_3 = 0.05$, $\gamma_1 = 0.1$, $\gamma_2 = 0.05$, $\mu = 0.05$, $\varepsilon = 0.1$, and $b = 0.05$. It is easily obtained that $R_0 = 1.5 > 1$. According to the Formulas (4) to (6), we know $S(\infty) = 0.667$, $E(\infty) = 0.111$, $I_1(\infty) = 0.056$, and $I_2(\infty) = 0.028$. The simulation results conform to Theorems 3 and 4, as shown in Figure 3.

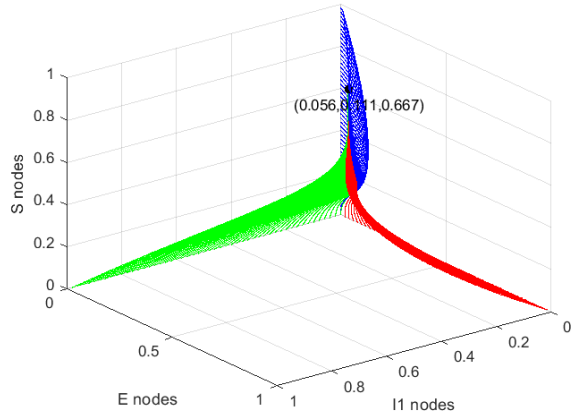

(**a**) The evolution of *S*, *E* and I_1 nodes

(Start from the *X*, *Y* and *Z* axis)

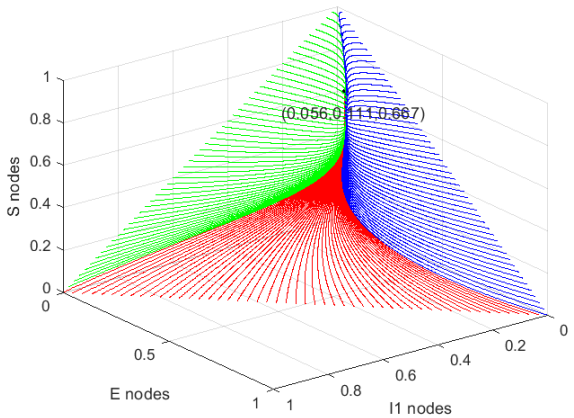

(**b**) The evolution of *S*, *E* and I_1 nodes

(Start from the hypotenuse)

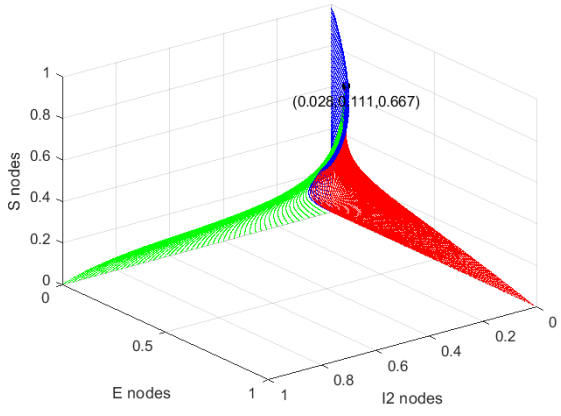

(**c**) The evolution of *S*, *E* and I_2 nodes

(Start from the *X*, *Y* and *Z* axis)

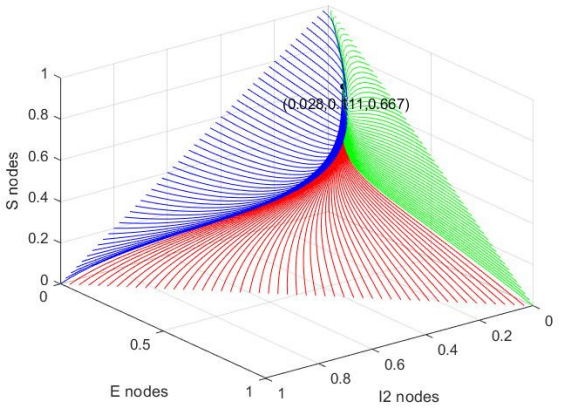

(**d**) The evolution of *S*, *E* and I_2 nodes

(Start from the hypotenuse)

Figure 3. The evolution of state variables when R_0 >1.

The assumptions are the same as in Figure 2. In Figure 3a,b, I_1 nodes ratio is the X-axis; the E nodes ratio is the Y-axis; and the S node ratio is the Z-axis. The simulation results show that the curve converges to (0.056, 0.111, 0.667) from the axis and the hypotenuse, respectively. In Figure 3c,d, I_2 nodes ratio is the X-axis; E nodes ratio is the Y-axis; and S node ratio is the Z-axis. The simulation results show that the curve converges to (0.028, 0.111, 0.667) from the axis and the hypotenuse, respectively.

4.3. Optimal Control

In this subsection, four parts will be considered: the evolution of sensor nodes, the total cost, the evolution of control variables, and the influence of control variables on R_0. Suppose that except for b = 0.1, the other parameters remain unchanged, as described in Section 4.2. Besides, set $\gamma(t) = \{\gamma_1(t), \gamma_2(t)\}$,$X(t) = \{S(t), E(t), I_1(t), I_2(t), R(t)\}$, $\beta(t) = \{\beta_1(t), \beta_2(t), \beta_3(t), \beta_4(t)\}$, $t_f = 200$, $c_1 = 1$, $c_2 = 2$, $S(0) = 0.4$, $E(0) = 0.3$, $I_1(0) = 0.2$, $I_2(0) = 0.1$, and $R(0) = 0$. The optimal control calculation process is shown in Figure 4.

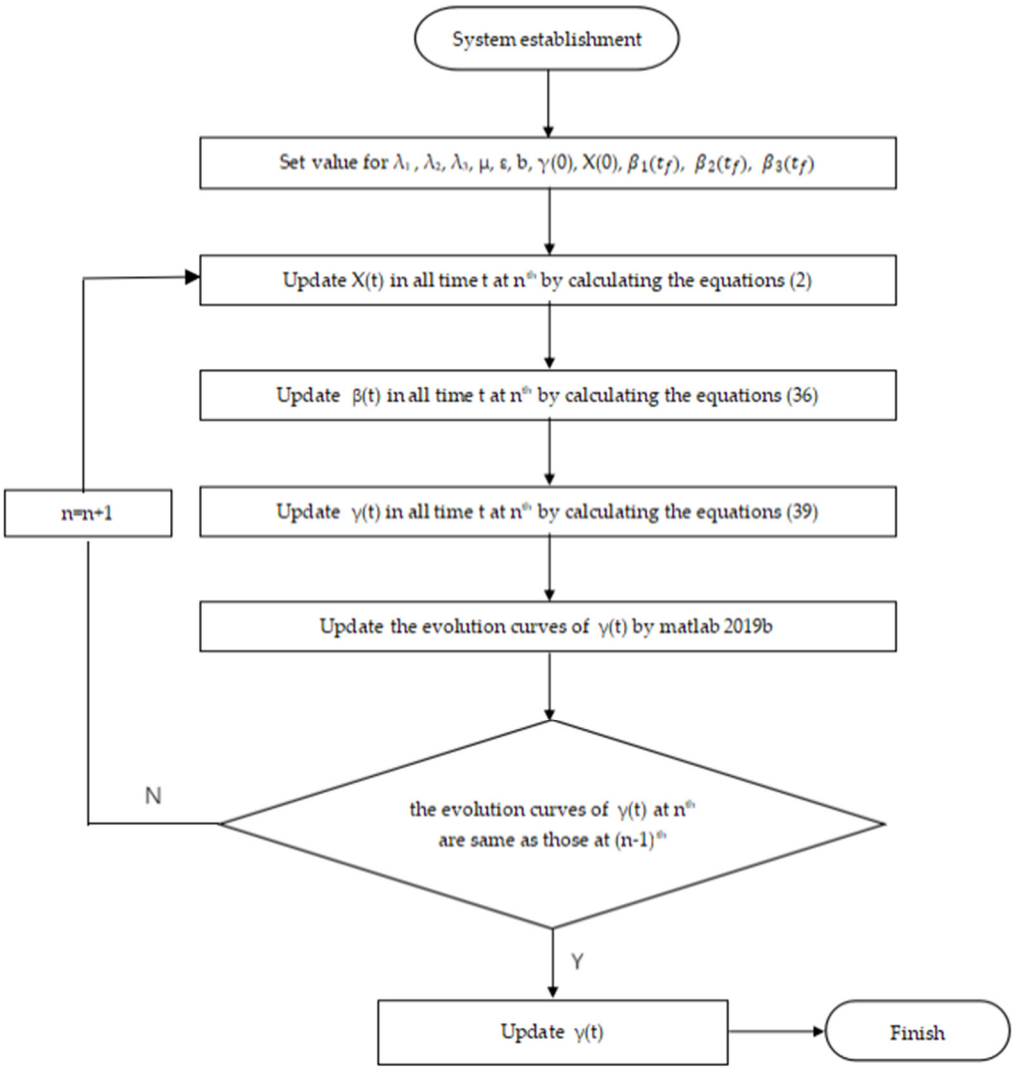

Figure 4. Flow chart of optimal control calculation.

Firstly, the control variables γ_1, γ_2 are be given an initial guess, and then Runge–Kutta method is used to solve the numerical solution of the state variables of the system (2). With the values of the obtained state variables, the initial values of the optimization variables and transversal conditions, the numerical solutions of the costate differential Equation (36)

are obtained by inverse integral. In order to better curb the spread of the virus, the value of control is always one when calculating the covariate. Finally, the values of the optimization control variables are obtained according to the Equation (39). Repeat the above process until the curves of the control variable are no longer changed.

4.3.1. Evolution of Sensor Nodes

In this part, we will discuss the evolution of sensor nodes under non-optimal control and optimal control, as shown in Figure 5.

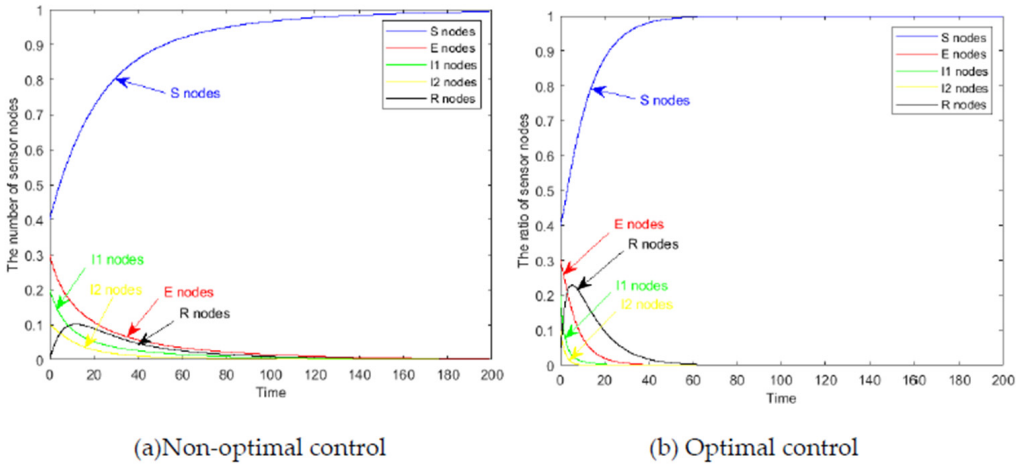

Figure 5. Evolution of sensor nodes under non-optimal control and optimal control.

One of our optimization objectives is to effectively control the ratio of nodes with virus at the terminal moment. By comparing Figures 5b and 5a, it can be seen that the nodes with virus under the optimal control are eliminated faster than those with fixed repair rate.

4.3.2. Total Cost and Control Variables

Another control goal is to reduce the repair cost on the basis of curbing the spread of the virus. The actual total cost of repair equation is $C = \int_0^{t_f}[c_1\gamma_1(t) + c_2\gamma_2(t)] \quad dt$. In this subsection, the fixed repair rates of 1 was selected as the non-optimal control group. By applying for approximate method, the total cost as shown in Figure 6.

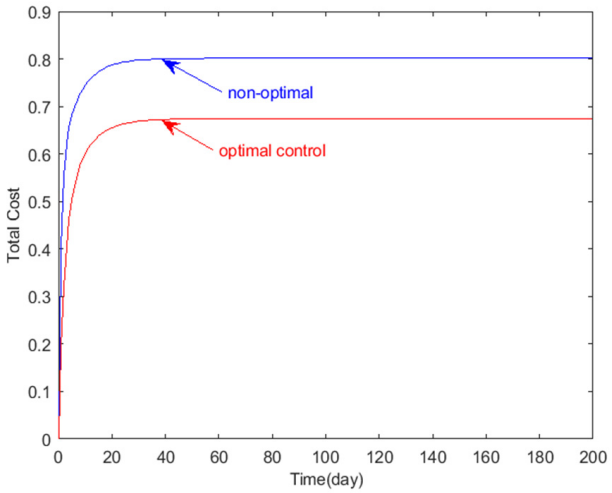

Figure 6. Total cost under optimal control and non-optimal control.

When γ_1 and γ_2 are always 1, the ratio of nodes with virus decreases fastest, the evolution of sensor nodes as shown in Figure 7 is similar to the evolution of sensor nodes

under the optimal control as shown in Figure 4a. It further shows that the goal of effectively controlling the ratio of nodes with virus is achieved. In addition, as shown in Figure 6, it can be seen that the total cost under the optimal control is lower than the total cost under non-optimal control. Specifically, the cost finally reaches 0.801 under the non-optimal control and the cost finally reaches 0.674 under optimal control. Therefore, the optimal strategy not only effectively controls the spread of the virus, but also minimizes the cost of the security strategy.

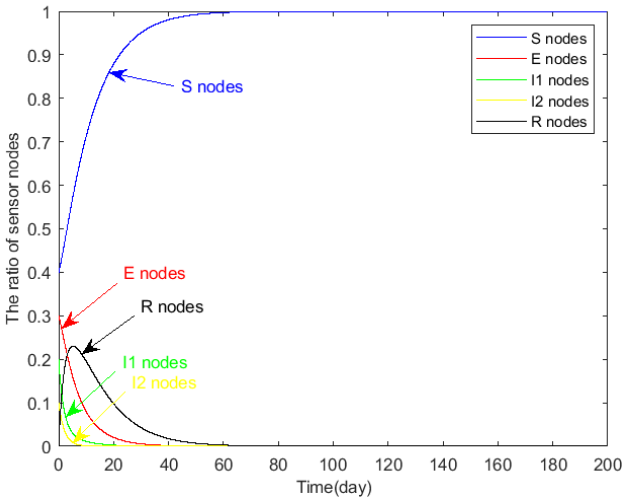

Figure 7. Evolution of sensor nodes when $\gamma_1 = \gamma_2 = 1$.

The results of optimizing variables are shown in Figure 8. In the early stage of security measures, because the ratio of I_1 nodes is higher and the repair cost c_2 of I_2 nodes is larger than the repair cost c_1 of I_1 nodes, so $\gamma_2 < \gamma_1$. Then, due to the decreasing ratio of I_1 nodes and the higher transmission rate λ_2 of I_2 nodes, I_2 nodes become the biggest threat, so $\gamma_2 > \gamma_1$. In the later stage, our goal is to diminish the number of nodes with virus, so the removal intensity of nodes with virus should be improved to make $\gamma_1 = \gamma_2 = 1$. Figure 8 provides the optimal combination of I_1 nodes repair rate γ_1 and I_2 nodes repair rate γ_2 at all times.

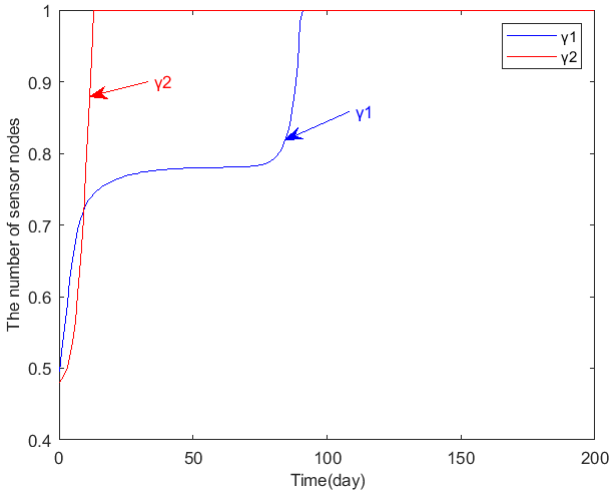

Figure 8. Evolution of control variables.

4.3.3. Influence of Control Variables on the Basic Reproduction Number R_0

The influence of control variables on R_0 is shown in Figure 9. The simulation results show that R_0 decreases with the increase of the repair rate γ_1 and γ_2. The lower the R_0,

the faster the virus is eliminated. When the control variables converge to 1, then $R_0 < 1$, as shown in Figure 8. Thus, the system will eventually achieve the disease-free equilibrium under optimal control. In addition, compared to γ_2, γ_1 has a greater impact on R_0 under these parameters as described in Section 4.3.

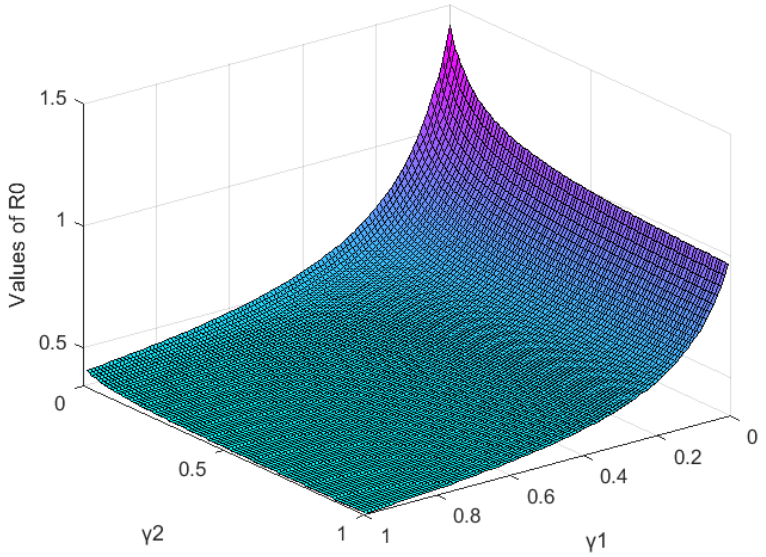

Figure 9. Influence of control variables on the basic reproduction number R_0.

5. Conclusions

In this paper, we use epidemiology to propose an improved SEIR model based on virus mutation, where E nodes are infectious and cannot be repaired to S nodes or R nodes, describing the propagation of mutated virus in WRSNs. Meanwhile, the basic reproduction number of the improved model is calculated by the next generation matrix method and the local and global stability of the two equilibrium points are proved by analyzing the stability of the model. Besides, in order to minimize the ratio of nodes with virus and the total cost associated with the measure, an optimal control strategy is proposed by optimizing the combination of the repair rates γ_1 and γ_2. In addition, the influence of control variables on the basic reproduction number is analyzed.

The simulation results verify the correctness of the stability theory. Further, the optimal control strategy is proved to be effective in controlling the ratio of nodes with virus and minimizing the maintenance cost. Figure 9 shows that the virus can be eliminated by adjusting the repair rate γ_1 and γ_2, but it needs to rise to a certain threshold. The SEIR propagation model with the mutated virus provides new insights into the virus propagation in WSNs. However, our model only considers one case of mutated virus, which is not comprehensive enough. In the future work, we will consider the case of time delay, and apply stochastic modeling and advanced mathematical theory when the ability permits. We hope the work of this paper can give some enlightenment to the relevant researchers.

Author Contributions: Conceptualization, G.L., J.C., Z.P. and J.L.; methodology, G.L., J.C., Z.P. and J.L.; software, G.L., J.C. and J.L.; validation, G.L. and J.C.; formal analysis, G.L. and J.C.; investigation, G.L., J.C. and Z.L.; writing—original draft preparation, J.C.; and writing—review and editing, G.L., J.C. and Z.L. All authors have read and agreed to the published version of the manuscript.

Funding: The author acknowledges funding received from the following science foundations: The National Natural Science Foundation of China (61403089, 51975136, 51575116, U1601204, 52075109), The 2020 Department of Education of Guangdong Province Innovative and Strong School Project (Natural Sciences)—Young Innovators Project (Natural Sciences) under Grant 2020KQNCX054, National Key Research and Development Program of China (2018YFB2000501), The Science and Technology Innovative Research Team Program in Higher Educational Universities of Guangdong Province (2017KCXTD025), The Innovative Academic Team Project of Guangzhou Education System

(1201610013), The Special Research Projects in the Key Fields of Guangdong Higher Educational Universities (2019KZDZX1009), The Science and Technology Research Project of Guangdong Province (2017A010102014, 2016A010102022), and The Science and Technology Research Project of Guangzhou (201707010293) are all appreciated for supporting this work.

Institutional Review Board Statement: Not applicable.

Informed Consent Statement: Not applicable.

Data Availability Statement: Not applicable.

Conflicts of Interest: The authors declare no conflict of interest.

References

1. Akyildiz, I.; Su, W.; Sankarasubramaniam, Y.; Cayirci, E. Wireless sensor networks: A survey. *Comput. Netw.* **2002**, *38*, 393–422. [CrossRef]
2. Liang, C.-J.M.; Musăloiu, E.R.; Terzis, A. Typhoon: A reliable data dissemination protocol for wireless sensor networks. In *Wireless Sensor Networks*; Verdone, R., Ed.; Springer: Berlin/Heidelberg, Germany, 2008; Volume 4913, pp. 268–285.
3. Lenin, R.B.; Ramaswamy, S. Performance analysis of wireless sensor networks using queuing networks. *Ann. Oper. Res.* **2013**, *233*, 237–261. [CrossRef]
4. Rashid, B.; Rehmani, M.H. Applications of wireless sensor networks for urban areas: A survey. *J. Netw. Comput. Appl.* **2016**, *60*, 192–219. [CrossRef]
5. Rasheed, A.; Mahapatra, R.N. The three-tier security scheme in wireless sensor networks with mobile sinks. *IEEE Trans. Parallel Distrib. Syst.* **2010**, *23*, 958–965. [CrossRef]
6. Reina, D.; Toral, S.; Johnson, P.; Barrero, F. A survey on probabilistic broadcast schemes for wireless ad hoc networks. *Ad Hoc Netw.* **2015**, *25*, 263–292. [CrossRef]
7. De, P.; Liu, Y.; Das, S. An epidemic theoretic framework for vulnerability analysis of broadcast protocols in wireless sensor networks. *IEEE Trans. Mob. Comput.* **2008**, *8*, 413–425. [CrossRef]
8. Zanero, S. Wireless malware propagation: A reality check. *IEEE Secur. Priv. Mag.* **2009**, *7*, 70–74. [CrossRef]
9. Yan, G.; Eidenbenz, S. Modeling propagation dynamics of bluetooth worms (extended version). *IEEE Trans. Mob. Comput.* **2008**, *8*, 353–368. [CrossRef]
10. Agapow, P.M. Computational brittleness and the evolution of computer viruses. In *International Conference on Parallel Problem Solving from Nature*; Springer: Berlin/Heidelberg, Germany, 1996; pp. 1–11.
11. Jia, X.; Xiong, X.; Jing, J.; Liu, P. Using purpose capturing signatures to defeat computer virus mutating. In *International Conference on Information Security Practice and Experienceeless*; Springer: Berlin/Heidelberg, Germany, 2010; pp. 153–171.
12. Li, D.; Li, C.; Xu, Y. The stability of a class of SEIR epidemic model with virus mutate. *Harbin Sci. Technol.* **2014**, *19*, 106–109.
13. Gao, J.; Zhang, T. Analysis on an SEIR epidemic model with logistic death rate of virus mutation. *J. Math. Res. Appl.* **2019**, *39*, 43–52.
14. Rui, M.; Youping, Y. Global dynamics of an avian influenza A(H7N9) epidemic model with latent period and nonlinear recovery rate. *Comput. Math. Methods Med.* **2018**, *2018*, 1–11.
15. Yang, Y. Viral dynamics of an HIV model with pulse antiretroviral therapy and adherence. *J. Nonlinear Sci. Appl.* **2018**, *11*, 516–528. [CrossRef]
16. Kephart, J.; White, S. Directed-graph epidemiological models of computer viruses. In Proceedings of the 1991 IEEE Computer Society Symposium on Research in Security and Privacy, Oakland, CA, USA, 20–22 May 1991.
17. Kephart, J.; White, S. Measuring and modeling computer virus prevalence. In Proceedings of the 1993 IEEE Computer Society Symposium on Research in Security and Privacy, Oakland, CA, USA, 24–26 May 1993.
18. Murray, W. The application of epidemiology to computer viruses. *Comput. Secur.* **1988**, *7*, 139–145. [CrossRef]
19. Newman, M.E.J. Spread of epidemic disease on networks. *Phys. Rev. E* **2002**, *66*, 016128. [CrossRef] [PubMed]
20. Tang, S.; Mark, B.L. Analysis of virus spread in wireless sensor networks: An epidemic model. In Proceedings of the 2009 7th International Workshop on Design of Reliable Communication Networks, Washington, DC, USA, 25–28 October 2009; pp. 86–91. [CrossRef]
21. Mishra, B.K.; Keshri, N. Mathematical model on the transmission of worms in wireless sensor network. *Appl. Math. Model.* **2013**, *37*, 4103–4111. [CrossRef]
22. Mishra, B.K.; Srivastava, S.K. A quarantine model on the spreading behavior of worms in wireless sensor network. *Trans. IoT Cloud Comput.* **2014**, *2*, 1–12.
23. Zizhen, Z. Dynamics of an epidemic model of computer virus with delays. *J. Zhejiang Univ. Ed.* **2015**, *42*, 677–686.
24. Srivastava, P.K.; Ojha, R.P.; Sharma, K.; Awasthi, S.; Sanyal, G.; Sanya, G. Effect of quarantine and recovery on infectious nodes in wireless sensor network. *Int. J. Sens. Wirel. Commun. Control.* **2018**, *8*, 26–36. [CrossRef]
25. Mishra, B.K.; Tyagi, I. Defending against malicious threats in wireless sensor network: A mathematical model. *Int. J. Inf. Technol. Comput. Sci.* **2014**, *6*, 12–19. [CrossRef]

26. Zhu, L.; Zhao, H. Dynamical analysis and optimal control for a malware propagation model in an information network. *Neurocomputing* **2015**, *149*, 1370–1386. [CrossRef]
27. Batista, F.K.; Del Rey, A.M.; Queiruga-Dios, A. A new individual-based model to simulate malware propagation in wireless sensor networks. *Mathematics* **2020**, *8*, 410. [CrossRef]
28. Huang, D.-W.; Yang, L.-X.; Yang, X.; Wu, Y.; Tang, Y.Y. Towards understanding the effectiveness of patch injection. *Phys. A Stat. Mech. Its Appl.* **2019**, *526*, 120956. [CrossRef]
29. Zhang, Z.; Kundu, S.; Wei, R. A delayed epidemic model for propagation of malicious codes in wireless sensor network. *Mathematics* **2019**, *7*, 396. [CrossRef]
30. Liu, G.; Peng, B.; Zhong, X.; Lan, X. Differential Games of Rechargeable Wireless Sensor Networks against Malicious Programs Based on SILRD Propagation Model. *Complexity* **2020**, *2020*, 5686413. [CrossRef]
31. Zhu, L.; Zhou, M.; Zhang, Z. Dynamical analysis and control strategies of rumor spreading models in both homogeneous and heterogeneous networks. *J. Nonlinear Sci.* **2020**, *30*, 1–32. [CrossRef]
32. Ojha, R.P.; Srivastava, P.K.; Sanyal, G.; Gupta, N. Improved model for the stability analysis of wireless sensor network against malware attacks. *Wirel. Pers. Commun.* **2021**, *116*, 2525–2548. [CrossRef]
33. Shen, S.; Zhou, H.; Feng, S.; Liu, J.; Zhang, H.; Cao, Q. An epidemiology-based model for disclosing dynamics of malware propagation in heterogeneous and mobile WSNs. *IEEE Access* **2020**, *8*, 43876–43887. [CrossRef]
34. Schöneburg, E. Neural networks hunt computer viruses. *Neurocomputing* **1991**, *2*, 243–248. [CrossRef]
35. Rad, B.B. *Metamorphic Computer Virus Detection: Using Hidden Markov Model*; LAP Lambert: Saarbrücken, Germany, 2016; p. 276.
36. Liu, G.; Peng, B.; Zhong, X.; Cheng, L.; Li, Z. Attack-Defense Game between Malicious Programs and Energy-Harvesting Wireless Sensor Networks Based on Epidemic Modeling. *Complexity* **2020**, *2020*, 3680518. [CrossRef]
37. Guillén, J.D.H.; Del Rey, Á.M.; Vara, R.C. On the optimal control of a malware propagation model. *Mathematics* **2020**, *8*, 1518. [CrossRef]
38. Marinoschi, G. Identification and control of SARS-CoV-2 epidemic model parameters. *arXiv* **2009**, arXiv:2009.13470.
39. Khouzani, M.H.R.; Sarkar, S. Maximum damage battery depletion attack in mobile sensor networks. *IEEE Trans. Autom. Control.* **2011**, *56*, 2358–2368. [CrossRef]
40. Liu, G.; Peng, B.; Zhong, X. A novel epidemic model for wireless rechargeable sensor network security. *Sensors* **2020**, *21*, 123. [CrossRef] [PubMed]
41. Huang, Y.; Zhu, Q. A Differential game approach to decentralized virus-resistant weight adaptation policy over complex networks. *IEEE Trans. Control Netw. Syst.* **2019**, *7*, 944–955. [CrossRef]
42. Liu, G.; Peng, B.; Zhong, X. Epidemic Analysis of Wireless Rechargeable Sensor Networks Based on an Attack–Defense Game Model. *Sensors* **2021**, *21*, 594. [CrossRef]
43. Lyapunov, A.M. The general problem of the stability of motion. *Int. J. Control* **1992**, *55*, 531–534. [CrossRef]
44. Gubar, E.; Taynitskiy, V.; Zhu, Q. Optimal control of heterogeneous mutating viruses. *J. Games* **2018**, *9*, 103. [CrossRef]